

Experimentally Realizable C-NOT Gate in a Flux Qubit/Resonator System

Shiro Saito,^{1,*} Todd Tilma,^{2,†} Simon J. Devitt,² Kae Nemoto,² and Koichi Semba¹

¹*NTT Basic Research Laboratories, NTT Corporation,*

3-1 Morinosato-Wakamiya, Atsugi-shi, Kanagawa-ken 243-0198, Japan

²*National Institute of Informatics, 2-1-2 Hitotsubashi, Chiyoda-ku, Tokyo-to 101-8430, Japan*

(Dated: November 28, 2018)

In this paper we present an experimentally realizable microwave pulse sequence that effects a Controlled NOT (C-NOT) gate operation on a Josephson junction-based flux-qubit/resonator system with high fidelity in the end state. We obtained a C-NOT gate process fidelity of 0.988 (0.980) for a two (three) qubit/resonator system under ideal conditions, and a fidelity of 0.903 for a two qubit/resonator system under the best, currently achieved, experimental conditions. In both cases, we found that “qubit leakage” to higher levels of the resonator causes a majority of the loss of fidelity, and that such leakage becomes more pronounced as decoherence effects increase.

PACS numbers: 74.50.+r, 03.67.Lx, 85.25.Cp

I. INTRODUCTION

The basic requirements for a successful quantum computer have been expressed by David DiVincenzo nearly a decade ago.^{1,2} These five criteria, listed below, have been widely accepted as being the best road map for achieving realizable quantum computing by most research programs throughout the world:

1. A scalable physical system of well-characterized qubits.
2. The ability to initialize the state of the qubits to a simple fiducial state.
3. Long (relative) decoherence times, much longer than the gate-operation time.
4. A universal set of quantum gates.
5. A qubit-specific measurement capability.

At this time, there are various schemes being proposed to satisfy the above criteria and realize a quantum computer.³ At the few-qubit level, these schemes include those based on trapped ions,⁴ linear optics,^{5,6} and nuclear spins in liquid-state molecules.^{7,8} For the long-term prospects of scalability though, those schemes that utilize Josephson junction-based qubits⁹ have significant advantages with current solid-state manufacturing technology.

Since the initial breakthrough in the coherent manipulation of a single Josephson junction-based charge qubit nearly a decade ago,⁹ the experimental focus has mostly shifted to the creation, control, and subsequent manipulation of, multi-qubit entanglement in similar Josephson junction-based systems. For example, coherent oscillations between two qubits have been observed by using a fixed inter-qubit coupling.^{10,11,12} However, the fixed nature of the qubit-qubit coupling used in these experiments makes it difficult to scale up such circuits in the future. To overcome this problem, a fast switchable coupling between two qubits has been proposed^{13,14} and also demonstrated.¹⁵

Beyond direct qubit-qubit couplings, another solution is to make use of a quantum bus (qubus) as a coupler between qubits.^{16,17,18} Using the “qubus” concept, we can perform any two qubit operation, between any two qubits that are coupled to the bus, without using multiple swap gates, which are necessary in other systems using direct qubit-qubit coupling. In particular, harmonic oscillators formed by superconducting circuits seem to be a good candidate for a “qubus”-type coupler. Early experiments with such couplers have shown coherent oscillations between a qubit and the oscillator, which was made of lumped elements, namely capacitors and inductors.^{19,20} More recently, a distributed circuit, based on a coplanar waveguide resonator, attracted considerable attention as an oscillator because of its high quality factor (Q -factor) and impedance matching to other circuits.^{21,22} Furthermore, coherent quantum state transfer, between two Josephson junction-based qubits, via such a waveguide resonator, has been demonstrated in both the phase²³ and charge regime.²⁴ Lastly, more recently, two-qubit algorithms have been demonstrated in a two-transmon qubit/resonator system.²⁵

Because of the experimental viability of the “qubus” coupler concept, as well as its obvious advantages in scalability, we are using this paper to propose an experimentally realizable microwave pulse sequence that will enact a controlled NOT (C-NOT) gate between two superconducting flux qubits, which are coupled via a harmonic oscillator bus. This pulse sequence flux qubit/resonator design is complementary to other recently proposed systems,^{16,26} but stands apart due to its efficiency of operation and fidelity of its end state.

II. EXPERIMENTAL SYSTEM

One of the most promising solid state quantum computing elements is a superconducting flux qubit that typically consists of three Josephson junctions in a loop: Two of equal size, one smaller by a factor $\alpha \simeq 0.8$.²⁷ The sizes of the junctions are chosen so that the geo-

metric self-inductance of the loop is not physically relevant. The two lowest energy states of the qubit at the flux degeneracy point, usually denoted as $|0\rangle$ and $|1\rangle$, are superpositions of macroscopically distinct clockwise and counter-clockwise persistent current states. Repeated experiments over the past few years have shown that this type of flux qubit is a well-defined quantum system that can perform single-qubit rotations^{28,29,30,31,32} as well as achieve longer coherence times than other kinds of superconducting qubits.³⁰ However, we have to operate the flux qubit at the degeneracy point in order to enjoy the best coherence time because it is easily affected by a flux fluctuation apart from the degeneracy point.^{30,31,32}

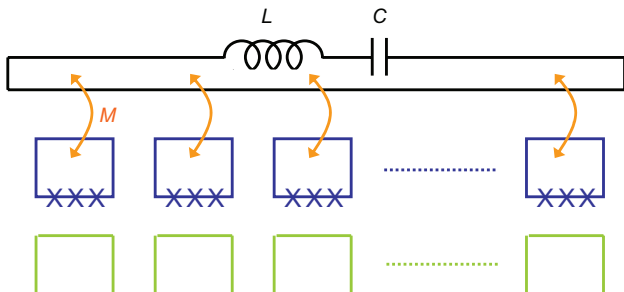


FIG. 1: (Color online) Multiple flux qubits (blue rectangles with three crosses), each addressed by its own microwave line (green line), coupled to a resonator via a mutual inductance M . The resonator is schematically represented by the inductor L and the capacitor C .

With the above in mind, we are currently working with the following architecture (see figure 1), built around the previously discussed three Josephson junction qubit design, which incorporates the fundamentals of the “qubus” concept.¹⁸ Each qubit couples to a resonator through a mutual inductance M . Here the resonator is schematically represented by lumped elements, but it can be a distributed circuit, for example, a coplanar strip waveguide. External magnetic flux through each qubit is a half flux quanta to set the qubits at the degeneracy point.

III. C-NOT PULSE SEQUENCE

In order to execute a C-NOT gate in our architecture (see figure 1) we have to entangle the flux qubits with the resonator. To do that, we need to apply a sequence of DC-shift pulses, or apply a sequence of microwave pulses, through microwave lines to our qubits. In the case of the former pulses, we can adiabatically change the qubit frequency to fit the resonator frequency, but also non-adiabatically to create a coupling between the qubit and the resonator. As a result, we can “turn on” the coupling between the qubit and the resonator non-adiabatically, making them into an entangled state.^{20,23} However, these pulses cause DC-based excursions away from the flux de-

generacy point, and can reduce the dephasing times of the qubits drastically. The large bandwidth of the pulses can also reduce the overall gate fidelity. Fortunately, a special flux qubit design may solve these problem by using elaborate DC pulses.²⁶

In the case of the latter pulses, we can create entanglement between the qubits and the resonator by using a known two-photon blue sideband (BSB) transition at the qubit’s degeneracy point.^{16,33} These microwave pulses have a more narrower bandwidth than the DC-shift pulses, thus allowing us to obtaining a much higher fidelity gate, as well as minimizing pulse-induced dephasing. C-NOT gate operations based on such BSB transitions have been achieved with a high fidelity in ion trap experiments.^{34,35} In these experiments, an elaborate controlled- Z gate, using four BSB pulses, was used.⁴

It is an interesting idea to introduce such a BSB-based C-NOT gate operation to our superconducting qubit/resonator system. However, it is hard to achieve a similar high fidelity because of the strong fixed coupling between the qubit and the resonator. This coupling leads to larger energy shifts at higher energy levels [see figure 2(a)]. Indeed, the BSB-based C-NOT gate uses up to $n = 2$ states, where n is the photon number in the resonator. Therefore, we will utilize this coupling to realize a high-fidelity controlled- Z gate instead by only using up to $n = 1$ states. From this, we can build a pulse sequence that will do a C-NOT gate [figure 2(b)].

As figure 2(b) shows, the first BSB π pulse transfers information from the control qubit to the resonator, and the second one transfers the information back to the control qubit. During a free evolution between the two pulses, we use only four energy levels, $|10\rangle$ and $|11\rangle$, for $n = 0$ and $n = 1$, where $|CT\rangle = |C\rangle|T\rangle$ and $|C\rangle$ ($|T\rangle$) represents the state of the control (target) qubit. The energy difference of the target qubit between $n = 0$ and $n = 1$ indicated by the two dashed arrows in figure 2(a) enable us to realize a controlled- Z gate between the resonator and the target qubit with a suitable temporal delay between the two pulses. Similar gate operations have been employed in nuclear magnetic resonance quantum computation.³⁶ These pulses, with proper phases, work as a controlled- Z gate between the two qubits (U_{CZ}). We have to adjust the phase difference between the two pulses carefully to cancel the effect of the off-resonant ac-Stark shift δ in figure 2(a).¹⁶ Finally, four single-qubit gates, and the U_{CZ} gate, form the C-NOT gate (U_{C-NOT}) as follows:

$$U_{C-NOT} = Y_C^{-2} Y_T U_{CZ} Y_T^{-1} Y_C^{-2} = - \begin{pmatrix} 0 & 1 & 0 & 0 \\ 1 & 0 & 0 & 0 \\ 0 & 0 & 1 & 0 \\ 0 & 0 & 0 & 1 \end{pmatrix} \quad (1)$$

in the two-qubit basis $\{|11\rangle, |10\rangle, |01\rangle, |00\rangle\}$. Here, Y_C and Y_T represent a $\frac{\pi}{2}$ rotation of the control qubit, and that of the target one, respectively.

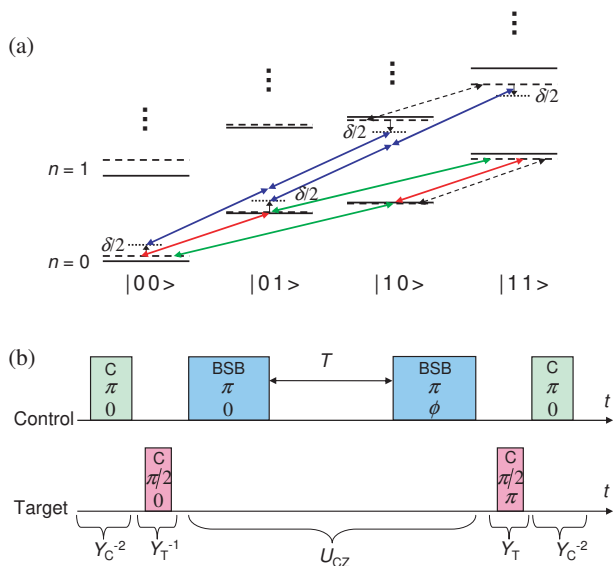


FIG. 2: (Color online) (a) Energy levels of the two qubit/resonator system and transitions used in our pulse sequence. Solid (dashed) lines represent the energy levels with (without) the coupling between the qubits and the resonator. Additional shifts δ occur during the irradiation of the BSB pulse. Energy difference between the dashed arrows is utilized to perform the controlled- Z gate between the resonator and the target qubit. (b) Basic operational sequence of “target,” “control,” and BSB pulses on our two qubits, using values defined in section IV A, that enact a C-NOT gate in our system. Each pulse is represented by the microwave frequency (Carrier frequency or BSB frequency), the rotation angle, and the phase of the microwave pulse. Note that the parameters T , the free evolution time, and ϕ , the microwave pulse phase, are variable: They are defined by the experimental system to those values that optimize the operation of the gate.

IV. NUMERICAL SIMULATIONS

As has been noted recently,²⁶ in order to accomplish our C-NOT, or any usable quantum computational gate, it will be necessary to manipulate multiple numbers of two-level quantum states, which will be our physical qubits, at will with some type of pulse sequence. For our system, as discussed in section III, and schematically represented in figure 1, this means that any single- or multi-qubit gate operation will be done using π pulses, $\frac{\pi}{2}$ pulses, and so on, most likely delivered by an on-chip microwave line, or lines. Our architecture not only achieves this, but also allows for a Hamiltonian representation that easily allows us to simulate whatever necessary pulse sequences we see fit to enact. In this section, our focus will be on simulating those pulses that implement our high-fidelity C-NOT gate upon any two qubits in the architecture.

To begin, when all the qubits in our system are at their respective degeneracy points, the overall system is

represented by the following Hamiltonian:

$$H = hf_{\text{res}}a^\dagger a + \sum_k \left(\frac{1}{2}hf_k\sigma_{z,k} + hg_k\sigma_{x,k}(a^\dagger + a) \right) + hA_{\text{MW},k} \sin(\omega_k t + \phi_k)\sigma_{x,k}. \quad (2)$$

Here, h is the Plank constant, f_{res} is the frequency of our resonator, $\frac{1}{2}hf_k\sigma_{z,k}$ represents our “k-th” qubit, $hg_k\sigma_{x,k}(a^\dagger + a)$ is the coupling term between the “k-th” qubit and the resonator, and $hA_{\text{MW},k} \sin(\omega_k t + \phi_k)\sigma_{x,k}$ describes the microwave pulse for each qubit. Since we are only looking at C-NOT gates, we will define one qubit as the “target,” and one as the “control” qubit. Lastly, we should note that, in principle, our gate operation uses only the ground, and first excited state, of the resonator.

Now, because we are wanting to analyze the time-evolution of multiple qubits - in particular, whether or not our pulse sequence accurately describes a C-NOT process on any two of them - we naturally will want to work within the density matrix formalism. In more detail, our simulated two-qubit gate, including error sources, is properly described by a completely positive map ε , the density matrix of the output state ρ_{out} of which can be written in the operator sum representation as³⁷

$$\rho_{\text{out}} = \varepsilon(\rho_{\text{in}}) = \sum_{m,n} \tilde{E}_m \rho_{\text{in}} \tilde{E}_n^\dagger \chi_{mn}, \quad (3)$$

where \tilde{E}_m are operators forming a basis in the space of 4×4 matrices and ρ_{in} is the density matrix of the input state. This expression shows that ε can be completely described by a complex number matrix, χ , once the set of operators \tilde{E}_m has been fixed.

In this work, we have chosen these 16 operators to be

$$\tilde{E}_{4i+j} = A_i \otimes A_j \quad (4)$$

in the case of a two-qubit gate. Here, $A_0 = I$, $A_1 = \sigma_x$, $A_2 = \sigma_y$, and $A_3 = \sigma_z$. To determine χ , which is a 16×16 matrix, we need to simulate our gate for 16 linearly independent input states $|\psi_{\text{in}}\rangle$. For these states we have chosen

$$|\psi_{\text{in}}\rangle = |\psi_i\rangle \otimes |\psi_j\rangle, \quad (5)$$

$$|\psi_i\rangle \in \{ |0\rangle, |1\rangle, (|0\rangle + |1\rangle)/\sqrt{2}, (|0\rangle + i|1\rangle)/\sqrt{2} \}$$

as the initial states. From this we can “measure” the gate fidelity using the process fidelity

$$F_p = \text{Tr}(\chi_{\text{ideal}}\chi_{\text{sim}}), \quad (6)$$

where χ_{ideal} and χ_{sim} represent the ideal matrix, and the one obtained from the simulation, respectively.

A. Simulation Parameters

Our two qubits (the “target” and “control”) and resonator operating frequencies, as well as couplings, were

defined in the following way:

$$\begin{aligned} f_1 &= f_{\text{Control}} = 6 \text{ GHz} & g_1 &= 0.1 \text{ GHz} \\ f_2 &= f_{\text{Target}} = 5 \text{ GHz} & g_2 &= 0.1 \text{ GHz} \\ f_{\text{res}} &= 10 \text{ GHz}. \end{aligned} \quad (7)$$

We then generated numerical simulations of equation (3) using the following values for our target and control pulses:

$$\begin{array}{ll} \text{TARGET PULSE} & \text{CONTROL PULSE} \\ A_{\text{MW},2} = 0.1 \text{ GHz} & A_{\text{MW},1} = 0.1 \text{ GHz} \\ \omega_2/2\pi = 4.99875 \text{ GHz} & \omega_1/2\pi = 5.9981 \text{ GHz} \\ \phi = 0 \text{ or } \pi & \phi = 0, \end{array} \quad (8)$$

as well as our blue-side-band (BSB) pulses:

$$\begin{array}{l} \text{CONTROL BSB} \\ A_{\text{MW},1} = 2 \text{ GHz} \\ \omega_1/2\pi = 7.5601 \text{ GHz} \\ \phi = 0 \text{ or } 0.34\pi. \end{array} \quad (9)$$

Here the rise/fall time of each pulse was set at 0.8 ns and the duration of the carrier $\pi(\frac{\pi}{2})$ -pulse was set at 5(2.5) ns. As we mentioned in section III, we optimized the duration of the BSB pulse, the free evolution time T , and the phase of the second BSB pulse ϕ in order to achieve the best gate fidelity; obtaining 16.295 ns, 162.865 ns and 0.34π , respectively. The total length of the pulse sequence is about 200 ns, which is much shorter than the reported coherence time of a flux qubit.³⁰ Lastly, we assumed that the first five resonator levels were accessible, thus $n = 0$ to $n = 4$, where n is the photon number in the resonator.

V. OBSERVATION AND ANALYSIS

Multiple simulations, using the previously defined parameters with various pulse shapes and operation times, have yielded an experimentally realizable matrix of target, control and BSB pulse sequences, represented in figure 2(b), that will initiate a C-NOT gate upon our two qubit/resonator system with high process fidelity, $F_p = 0.988$, and within the coherence time of known flux qubit systems. The computed gate is as follows (to four significant figures):

$$U'_{\text{C-NOT}} = \begin{pmatrix} 0.0001 & 0.9863 & 0.0013 & 0.0022 \\ 0.9863 & 0.0001 & 0.0020 & 0.0013 \\ 0.0021 & 0.0014 & 0.9886 & 0.0034 \\ 0.0013 & 0.0023 & 0.0035 & 0.9880 \end{pmatrix}. \quad (10)$$

We also evaluated the effects of decoherence on our C-NOT gate by introducing a linear loss to the resonator (quality factor Q), as well as relaxation rates Γ_1 and dephasing rates Γ_2 to the qubits, via a master equation of

the Lindblad form (see figures 3 and 4). Here we assumed that Γ_1 and Γ_2 for both qubits were equal. We obtained a process fidelity of 0.903 in the best conditions which have been achieved experimentally, for example, $Q = 10^6$, $\Gamma_1 = \Gamma_2 = 0.25$ MHz. Although the fidelity without the decoherence is not unity, it is much better than that with the decoherence, hence our pulse sequence could be useful enough to demonstrate the C-NOT gate experimentally.

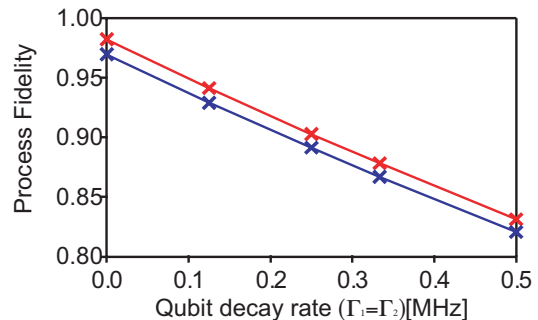


FIG. 3: (Color online) Process fidelity as a function of qubit decay rate. The upper (lower) curve represents the fidelity when the quality factor of the resonator is 10^6 (3×10^5).

Now, in the case of flux qubits, it is difficult to fabricate a qubit which has an exact designed gap frequency at the degeneracy point, unless using the qubit with a controllable third junction.³⁸ Hence, we also simulated the case in which the two qubit frequencies became closer to each other. When $f_{\text{res}} = 10$ GHz and $f_{\text{Control}} = 6$ GHz and $f_{\text{Target}} = 5.5$ GHz, we obtained a process fidelity of 0.986 without decoherence. Decreasing the difference between two qubit frequencies did not significantly affect the fidelity.

This gate also works with any two qubits in a system with many qubits, since we can decouple any unused qubits from the resonator via very quick (≈ 5 ns) π pulses applied at the center of the two BSB pulses. For example, we obtained an process fidelity of $F_p = 0.980$ in a three qubit/resonator system where the frequency of the third unused qubit was 7 GHz, its coupling to the resonator was 0.1 GHz, and the microwave frequency of the decoupling pulse was 6.9973 GHz. The other system conditions were similar to that use in the two-qubit simulation.

Unfortunately, our gate fidelity, while still better than that currently achieved by other experimental systems (see for example Riebe *et al.* and their table II),³⁵ is still not unity. The lack of unit fidelity in our C-NOT gate is due to “qubit leakage”; the unintended, and persistent, excitation of higher-order resonator levels. As Fazio *et al.* noted in 2000,³⁹ qubit leakage issues are due to the fact that the qubit Hilbert space is actually a subspace of a larger Hilbert space; in our case, one that includes accessible higher-order resonator levels. Although their work focused on charge qubits, their basic conclusions

hold for flux qubits as well, as our simulations have shown (see figure 4).

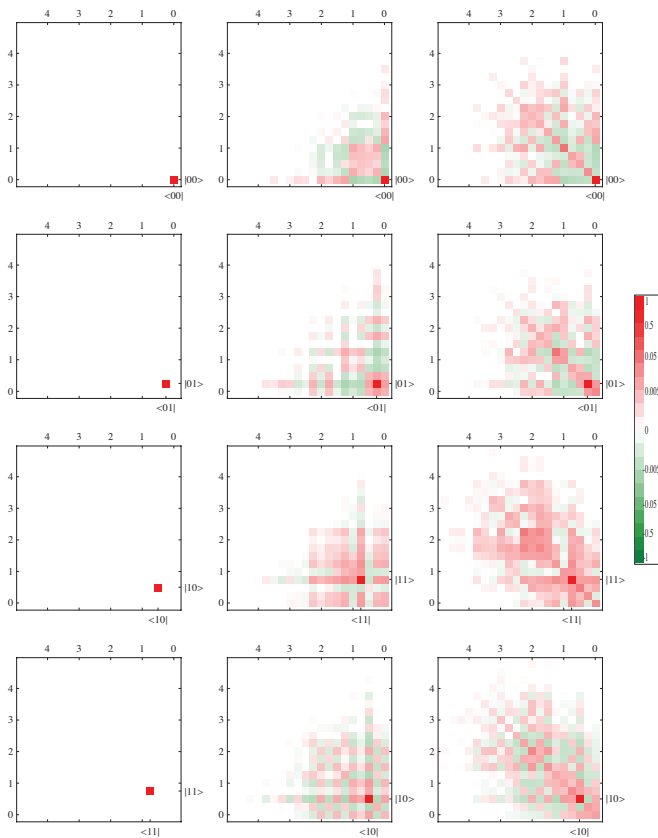


FIG. 4: From top: Initial (left) and final (middle and right) density matrices (real components only) showing the $|00\rangle \mapsto |00\rangle$, $|01\rangle \mapsto |01\rangle$, $|10\rangle \mapsto |11\rangle$, and $|11\rangle \mapsto |10\rangle$ operations, and the corresponding qubit leakage into higher resonator modes ($n > 0$), due to the pulse sequence values defined in section IV A, without and with decoherence ($Q = 10^6$, $\Gamma_1 = \Gamma_2 = 0.25$ MHz). The color scheme used is a nonlinear gradient: Zero values are white, with negative values greenish and positive values reddish.

In more detail, coherent leakage into higher order modes of the harmonic oscillator bus seems to be responsible for the missing process fidelity of the system. Not only is this large an error rate unacceptable from the standpoint of large scale, fault-tolerant quantum computation, but the error channel itself is problematic to correct under current quantum error correction (QEC) schemes.

One of the fundamental assumptions of QEC is that errors affecting qubits are localized to the two-levels associated with the qubit encoding. Once errors begin to violate this assumption, either through state leakage or actual qubit loss, additional mechanisms must be employed, at the encoding level, to allow for correction. Many different techniques have been developed to compensate for this type of error channel, including leakage

protection through non-demolition detection and state re-injection,^{40,41,42,43} correction by teleporting “leaked” qubits back into the 2-level subspace,⁴⁴ and specialized leakage reduction units (LRU’s) which suppress leakage through a pulse sequences in a similar manner to bang-bang protection for qubit dephasing.^{45,46} Unfortunately, these techniques are quite cumbersome and involve specialized protocols that go beyond the standard operations to realize QEC.

Ideally, for large scale qubit applications, we do not want to correct for qubit leakage, instead we wish to suppress it to a sufficient level where it can be ignored. It should be noted that this requirement is not as trivial as it might appear. For large scale applications, fault-tolerant quantum computation requires extremely low error rates. This “target” error rate for fault-tolerant QIP, often referred to as the “fault-tolerant threshold” is highly dependent on the underlying physical architecture and can be anywhere between 10^{-3} and 10^{-7} .^{47,48} The important point to realize is that if we wish to ignore coherent leakage errors, and avoid implementing specialized protocols, errors caused by qubit leakage will need to be several orders of magnitude below any other correctable source of qubit error. Therefore, the pulse design of this bus mediated qubit/qubit coupling will be required to exhibit effectively zero leakage, even before open system quantum effects are even considered, if it is to be used to do realizable QIP. This means that a new pulse sequence will need to be created.

VI. FOLLOW-ON PULSE SEQUENCE POSSIBILITIES

From our work, it is our belief that the seen qubit leakage, even taking our simple decoherence model into account, and the corresponding non-unity fidelity is an unavoidable consequence of the programmed waveforms, and expected physical implementation, of our microwave pulses. Experimentally, in order to avoid qubit state transitions, the rise and fall times of our pulses have to be long enough to fulfill the adiabatic condition, but also short enough to avoid unwanted relaxation processes. Temporal lengths of the various target, control and BSB pulses used also depend on the microwave pulse amplitude, and are experimentally determined from the system’s driven Rabi oscillations. Thus, while these numerical simulations demonstrate the principal application of a bus-mediated controlled qubit/qubit interaction, the implementation of the proposed pulse sequence requires further improvement of the leakage to build up not only a several qubit system, from the standpoint of a quantum testbed, but also a really-scalable QIP system.

In more detail, analysis of our control, target and BSB pulse matrices indicates that our qubit leakage is initiated by our first BSB pulse on the control qubit. Since the second BSB pulse on the same qubit is only different by a phase, we only require a modified version of the BSB

pulse matrix to avoid leaking population into higher order modes of the harmonic oscillator. Also, as the simple “top hat” pulse design we have examined is already very well confined, it is expected that this pulse represents a good first approximation to a zero leakage modification, and due to the structure of this sequence, we already have a good idea which section of the pulse is “leaky.” Thus we feel that the only way to truly generate a microwave pulse-induced gate, with fidelity experimentally equivalent to unity, for this system will be to use technologies based on optimal quantum control.^{49,50,51,52,53}

Optimal quantum control is a vast area of theoretical and numerical techniques that were developed largely in the field of nuclear magnetic resonance (NMR) and quantum chemistry, in order to find complicated control fields for NMR manipulations, or to increase chemical yields in chemical reactions involving photonic reagents. This research has more recently been applied to the quantum information field,^{52,54,55,56,57} utilized to construct high-fidelity quantum gates from a set of classical controls, which may be pulsed in counter-intuitive ways, that would be difficult to find with traditional analytical techniques.

There are many different ways in which to formulate the optimal control problem, in terms of the target quantum operation, and in terms of numerical search methods. In a very broad way, the general idea of optimal control methods is to iteratively search for a target set of control field parameters that drive a system Hamiltonian in a controlled manner. Depending on the system considered, the target parameter could be quantum process fidelity, or operational time of the evolution, or the value of a specific quantum observable.

One such example of an optimal control method is the standard numerical algorithm known as gradient ascent pulse engineering (GRAPE),⁵¹ optimal quantum gates (in terms of process fidelity) are constructed by iteratively varying control parameters, and analytically calculating the gradient changes, in order to find the minimum fidelity points in the underlying unitary space. These techniques have been applied to ion traps,⁵⁶ vibrational modes in molecules,⁵⁵ as well as in the superconducting regime^{56,58} with significant success.

Our future work will involve utilizing these numerical techniques to find smooth control field parameters that modify the above simulated BSB pulse to one that eliminates leakage to higher order field modes. Hopefully, once we eliminate the final issue of qubit leakage, we will utilize these numerical algorithms in full open system calculations to develop high fidelity control pulses

for superconducting systems undergoing decoherence.

VII. CONCLUSIONS

Our simulations have confirmed a usable control, target, and BSB pulse matrix, as well as the required operational pulse rise/fall time envelope published previously,⁵⁹ for an experimentally successful microwave pulse-induced C-NOT gate. However they have also shown that this set of pulses, in particular the BSB set, incites unwanted qubit leakage, at a minimum, into the first and second excited states of the coupling resonator, which makes them troublesome for usage in a more QIP-focused architecture.

Our proposed solution to this problem, replacing the BSB pulse sequence with a sequence based on optimal quantum control concepts, seems to have the potential to reduce the observed qubit leakage. Yet it is still uncertain whether or not the required pulse sequences needed for these codes can be realized experimentally. The main reason is that our current architecture has a 1:1 resonance between qubit number and microwave lines. This was done in order to avoid cross-talk between qubits. More complicated pulse sequences on this architecture, such as those needed for GRAPE codes, run the risk of initiating cross-talk between qubits and other microwave lines, or exciting on-chip fluctuators close to, or within, each qubit’s junction.

Currently, we are planning to explore these issue in more detail by investigate other GRAPE-inspired multi-qubit/resonator gate sequences, as well as modifications to the architecture. Future work will also look into more accurately modeling the dynamical impact of the various low- and high- frequency noise sources inherent in our system,⁵⁹ using a more generalized open quantum system treatment.⁶⁰

VIII. ACKNOWLEDGMENTS

We would like to thank W. J. Munro, H. Nakano, T. P. Spiller, and J. E. Mooij for numerous, useful discussions and The Center for Complex Quantum Systems at The University of Texas at Austin for their continued support and encouragement. This work was supported in part by Grant-in-Aid for Scientific Research of Specially Promoted Research #18001002 by MEXT, Grant-in-Aid for Scientific Research (A) #18201018 by JSPS.

* email:s-saito@will.brl.ntt.co.jp

† email:ttilma@nii.ac.jp

¹ D. P. DiVincenzo, Science **270**, 255 (1995).

² D. P. DiVincenzo, Fortschr. Phys. **48**, 771 (2000).

³ T. P. Spiller, W. J. Munro, S. D. Barrett, and P. Kok,

Contemp. Phys. **46**, 407 (2005).

⁴ J. I. Cirac and P. Zoller, Phys. Rev. Lett. **74**, 4091 (1995).

⁵ E. Knill, R. Laflamme, and G. J. Milburn, Nature **409**, 46 (2001).

⁶ P. Kok, W. J. Munro, K. Nemoto, T. C. Ralph, J. P. Dowling,

- ing, and G. J. Milburn, *Rev. Mod. Phys.* **79**, 135 (2007).
- 7 D. G. Cory, A. F. Fahmy, and T. F. Havel, *Proc. Nat. Acad. Sci. USA* **94**, 1634 (1994).
 - 8 N. A. Gershenfeld and I. L. Chuang, *Science* **275**, 350 (1997).
 - 9 Y. Nakamura, Y. A. Pashkin, and J. S. Tsai, *Nature* **398**, 786 (1999).
 - 10 Y. A. Pashkin, T. Yamamoto, O. Astafiev, Y. Nakamura, D. V. Averin, and J. S. Tsai, *Nature* **421**, 823 (2003).
 - 11 R. McDermott, R. W. Simmonds, M. Steffen, K. B. Cooper, K. Cicak, K. D. Osborn, S. Oh, D. P. Pappas, and J. M. Martinis, *Science* **307**, 1299 (2005).
 - 12 J. H. Plantenberg, P. C. de Groot, C. J. P. M. Harmans, and J. E. Mooij, *Nature* **447**, 836 (2007).
 - 13 P. Bertet, C. J. P. M. Harmans, and J. E. Mooij, *Phys. Rev. B* **73**, 064512 (2006).
 - 14 A. O. Niskanen, Y. Nakamura, and J. S. Tsai, *Phys. Rev. B* **73**, 094506 (2006).
 - 15 A. O. Niskanen, K. Harrabi, F. Yoshihara, Y. Nakamura, S. Lloyd, and J. S. Tsai, *Science* **316**, 723 (2007).
 - 16 A. Blais, J. Gambetta, A. Wallraff, D. I. Schuster, S. M. Girvin, M. H. Devoret, and R. J. Schoelkopf, *Phys. Rev. A* **75**, 032329 (2007).
 - 17 H. Nakano, K. Kakuyanagi, M. Ueda, and K. Semba, *Appl. Phys. Lett.* **91**, 032501 (2007).
 - 18 T. P. Spiller, K. Nemoto, S. L. Braunstein, W. J. Munro, P. van Loock, and G. J. Milburn, *New J. Phys.* **8**, 30 (2006).
 - 19 I. Chiorescu, P. Bertet, K. Semba, Y. Nakamura, C. J. P. M. Harmans, and J. E. Mooij, *Nature* **431**, 159 (2004).
 - 20 J. Johansson, S. Saito, T. Meno, H. Nakano, M. Ueda, K. Semba, and H. Takayanagi, *Phys. Rev. Lett.* **96**, 127006 (2006).
 - 21 A. Wallraff, D. I. Schuster, A. Blais, L. Frunzio, R. S. Huang, J. Majer, S. Kumar, S. M. Girvin, and R. J. Schoelkopf, *Nature* **431**, 162 (2004).
 - 22 M. Hofheinz, E. M. Weig, M. Ansmann, R. C. Bialczak, E. Lucero, M. Neeley, A. D. O'Connell, H. Wang, J. M. Martinis, and A. N. Cleland, *Nature* **454**, 310 (2008).
 - 23 M. A. Sillanpää, J. I. Park, and R. W. Simmonds, *Nature* **449**, 438 (2007).
 - 24 J. Majer, J. M. Chow, J. M. Gambetta, J. Koch, B. R. Johnson, J. A. Schreier, L. Frunzio, D. I. Schuster, A. A. Houck, A. Wallraff, et al., *Nature* **449**, 443 (2007).
 - 25 L. DiCarlo, J. M. Chow, J. M. Gambetta, L. S. Bishop, D. I. Schuster, J. Majer, A. Blais, L. Frunzio, S. M. Girvin, and R. J. Schoelkopf, *arXiv:cond-mat/09032030* (2009).
 - 26 F. Brito, D. P. DiVincenzo, R. H. Koch, and M. Steffen, *New J. Phys.* **10**, 033027 (2008).
 - 27 J. E. Mooij, T. P. Orlando, L. Levitov, L. Tian, C. H. van der Wal, and S. Lloyd, *Science* **285**, 1036 (1999).
 - 28 I. Chiorescu, Y. Nakamura, C. J. P. M. Harmans, and J. E. Mooij, *Science* **299**, 1869 (2003).
 - 29 S. Saito, T. Meno, M. Ueda, H. Tanaka, K. Semba, and H. Takayanagi, *Phys. Rev. Lett.* **96**, 107001 (2006).
 - 30 P. Bertet, I. Chiorescu, G. Burkard, K. Semba, C. J. P. M. Harmans, D. P. DiVincenzo, and J. E. Mooij, *Phys. Rev. Lett.* **95**, 257002 (2005).
 - 31 F. Yoshihara, K. Harrabi, A. O. Niskanen, Y. Nakamura, and J. S. Tsai, *Phys. Rev. Lett.* **97**, 167001 (2006).
 - 32 K. Kakuyanagi, T. Meno, S. Saito, H. Nakano, K. Semba, H. Takayanagi, F. Deppe, and A. Shnirman, *Phys. Rev. Lett.* **98**, 047004 (2007).
 - 33 P. J. Leek, S. Filipp, P. Maurer, M. Baur, R. Bianchetti, J. M. Fink, M. Göppl, L. Steffen, and A. Wallraff, *arXiv:cond-mat/08122678* (2008).
 - 34 F. Schmidt-Kaler, H. Häffner, M. Riebe, S. Gulde, G. P. T. Lancaster, T. Deuschle, C. Becher, C. F. Roos, J. Eschner, and R. Blatt, *Nature* **422**, 408 (2003).
 - 35 M. Riebe, K. Kim, P. Schindler, T. Monz, P. O. Schmidt, T. K. Körber, W. Hänsel, H. Häffner, C. F. Roos, and R. Blatt, *Phys. Rev. Lett.* **97**, 220407 (2006).
 - 36 L. M. K. Vandersypen and I. L. Chuang, *Rev. Mod. Phys.* **76**, 1037 (2004).
 - 37 I. L. Chuang and M. A. Nielsen, *J. Mod. Opt.* **44**, 2455 (1997).
 - 38 F. G. Paauw, A. Fedorov, C. J. P. M. Harmans, and J. E. Mooij, *Phys. Rev. Lett.* **102**, 090501 (2009).
 - 39 R. Fazio, G. M. Palma, E. Sciacca, and J. Siewert, *Physica B* **284**, 1822 (2000).
 - 40 J. Preskill, *Introduction to Quantum Computation* (World Scientific, Singapore, 1998), pp. 213–269.
 - 41 M. Grassl, T. Beth, and T. Pellizzari, *Phys. Rev. A* **56**, 33 (1997).
 - 42 J. Vala, K. B. Whaley, and D. S. Weiss, *Phys. Rev. A* **72**, 052318 (2005).
 - 43 K. Khodjasteh and D. A. Lidar, *Phys. Rev. A* **68**, 022322 (2003).
 - 44 C. Mochon, *Phys. Rev. A* **69**, 032306 (2004).
 - 45 L. A. Wu, M. S. Byrd, and D. A. Lidar, *Phys. Rev. Lett.* **89**, 127901 (2002).
 - 46 M. S. Byrd, D. A. Lidar, L. A. Wu, and P. Zanardi, *Phys. Rev. A* **71**, 052301 (2005).
 - 47 P. Aliferis, F. Brito, D. P. DiVincenzo, J. Preskill, M. Steffen, and B. M. Terhal, *New J. Phys.* **11**, 013061 (2009).
 - 48 A. M. Stephens, A. G. Fowler, and L. C. L. Hollenberg, *Quantum Inf. Comput.* **8**, 330 (2008).
 - 49 R. S. Judson and H. Rabitz, *Phys. Rev. Lett.* **68**, 1500 (1992).
 - 50 V. F. Krotov, *Global Methods in Optimal Control Theory* (Marcel Dekker, New York, 1996).
 - 51 N. Khaneja, T. Reiss, C. Kehlet, T. Schulte-Herbrüggen, and S. J. Glaser, *J. Magn. Reson.* **172**, 296 (2005).
 - 52 T. Schulte-Herbrüggen, A. Spörl, N. Khaneja, and S. J. Glaser, *Phys. Rev. A* **72**, 042331 (2005).
 - 53 S. G. Schirmer, I. C. H. Pullen, and A. I. Solomon, *J. Opt. B: Quantum Semiclassical Opt.* **7**, S293 (2005).
 - 54 T. Schulte-Herbrüggen, A. Spörl, R. Marx, N. Khaneja, J. M. Myers, A. F. Fahmy, and S. J. Glaser, *Lectures on Quantum Information* (WILEY-VCH Verlag GmbH and Co. KGaA, Germany, 2007), chap. Quantum Computing Implemented via Optimal Control: Theory and Application to Spin and Pseudo-Spin Systems, pp. 481–501.
 - 55 C. M. Tesch and R. de Vivie-Riedle, *Phys. Rev. Lett.* **89**, 157901 (2002).
 - 56 P. Rebentrost and F. K. Wilhelm, *Phys. Rev. B* **79**, 060507(R) (2009).
 - 57 V. Nebendahl, H. Häffner, and C. F. Roos, *Phys. Rev. A* **79**, 012312 (2009).
 - 58 A. Spörl, T. Schulte-Herbrüggen, S. J. Glaser, V. Bergholm, M. J. Storcz, J. Ferber, and F. K. Wilhelm, *Phys. Rev. A* **75**, 012302 (2007).
 - 59 F. Deppe, M. Mariani, E. P. Menzel, S. Saito, K. Kakuyanagi, H. Tanaka, T. Meno, K. Semba, H. Takayanagi, and R. Gross, *Phys. Rev. B* **76**, 214503 (2007).
 - 60 C. A. Rodriguez-Rosario and E. C. G. Sudarshan, *arXiv:quant-ph/08031183* (2008).